inter.noise 2000
The 29th International Congress and Exhibition on Noise Control Engineering
27-30 August 2000, Nice, FRANCE

I-INCE Classification: 7.6

PREDICTION OF RATTLE NOISE FROM AN UNLOADED GEAR PAIR

T.-C. Kim, R. Singh

The Ohio State University, Acoustics and Dynamics Laboratory, Department of Mechanical Engineering and Center for Automotive Research, 43210-1107, Columbus, OH, United States Of America

Tel.: 614)292-3146 / Fax: 614)292-3163 / Email: kim.897@osu.edu

Keywords:

ABSTRACT

Clearance nonlinearities generate significant vibro-impacts and periodic-impulsive noise in many mechanical systems and vehicles. A particular problem for a manual transmission of a light duty truck is studied in this paper. Experimental measurements show that an unloaded gear pair in the drive mode induces the torsional rattle. Both neutral state and unloaded gear rattle problems are then simulated using new linear and nonlinear mathematical models. Results and trends predicted by the computer simulation model are used to understand experimental data and to examine the effects of dual-mass flywheel and drag torque.

1 - INTRODUCTION

Rattle noise is induced by gear backlashes and other clearance nonlinearities in many lightly loaded mechanical drive systems including manual transmissions of cars and trucks. Contemporary vehicle design trends toward lighter flywheels and lower idling speeds increase the likelihood of introducing gear rattle as a major noise source, especially from the perceived sound quality standpoint. Prior investigators have used a variety of simulation techniques to understand and predict such problems. Although some of the general characteristics of neutral gear rattle in automotive transmissions are known [1-3], no specific analytical models are available which can be used to understand the dynamic behavior of an unloaded gear pair in the drive rattle mode. Usually, conditions for the onset of vibro-impacts from unloaded gear pairs or splines are more favorable than rattle from an engaged gear pair. Consider a specific noise problem that occurs in a light truck that is equipped with a longitudinally installed V6 turbo diesel engine, rear wheel drive with two universal joints, and a five-speed dual-shaft manual transmission. The schematic of this transmission is shown in Figure 1. Initial experiments are defined to clarify the phenomena in a qualitative manner. All measurements are therefore compared to the same reference and differences between alternate rattle problems are noted.

Experiments under several conditions show significant and annoying rattle noises at lower engine speeds during light accelerations or coast conditions. However, the rattle noise can be heard in all engaged gear run-ups. Torsional velocity ($\dot{\theta}$, rpm) time histories are acquired via running this vehicle in first, second, and third gears. Afterwards, the $\dot{\theta}$ data are converted into accelerations ($\ddot{\theta}$), and the third, sixth, and ninth engine firing orders are removed. Results of the relative acceleration levels ($\ddot{\theta}_p$) on a peak-to-peak basis are shown in Table 1; the units of $\ddot{\theta}_p$ are omitted. Experiment clearly shows that the main rattle noise comes from unloaded gear pairs. The $\ddot{\theta}_p$ level of the overdrive gear pair is much higher than that from the engaged gear pair. This occurs in all gear run-up conditions. However, the nature of the underlying physical phenomena, including whether single-sided or double-sided impacts are generated, are not understood, based on the experimental study alone. Therefore, several mathematical models are developed. First, linear eigensolutions of the driveline are studied. Second, a corresponding reduced order nonlinear simulation model is developed. Finally, the roles of dual-mass flywheel and drag torque are numerically studied.

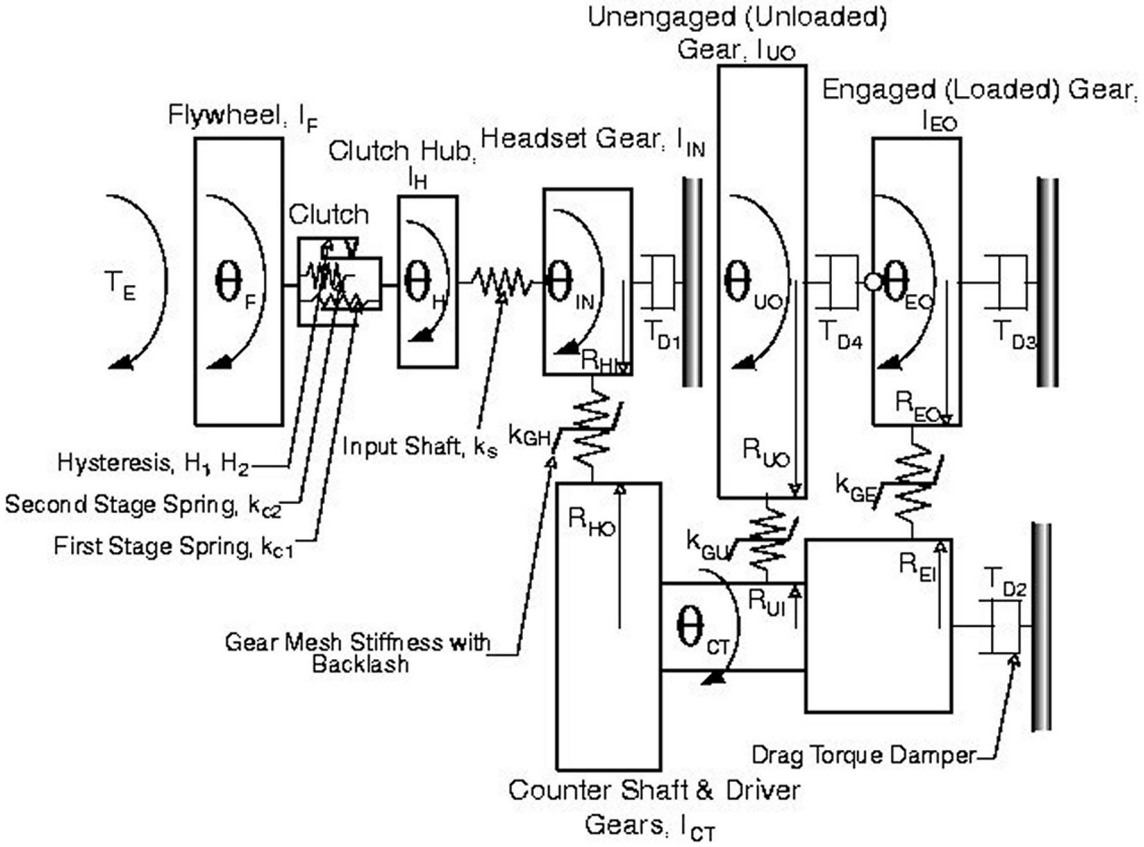

Figure 1: Schematic of a 6-degree of freedom torsional model.

Engine Speed	$\ddot{\theta}_p$ (peak to peak), consistent units		Noise perception
	Engaged pair (3rd)	Unloaded pair (Overdrive)	
850 rpm	400	1000	No rattle
950 rpm	800	6000	Severe rattle

Table 1: Relative acceleration levels ($\ddot{\theta}_p$) from the vehicle run-up experiments.

2 - SIMULATION MODELS

First, a linear time-invariant model of the transmission of Figure 1 is proposed. A 6-degree of freedom torsional model assumes the following: a. the clutch is engaged in the first or second stage, b. the hysteresis of the clutch is negligible, c. each shaft acts like a linear torsional spring (k_s), and d. the gear interface regime may be modeled by an equivalent mesh stiffness term [2]. Relevant inertial elements include flywheel and clutch friction pad (I_F), clutch hub (I_H), input shaft and headset driver (I_{IN}), counter shaft with all driver and output gears "welded" on it except the unloaded gear (I_{CT}), engaged output gear and output shaft (I_{EO}), and unloaded output gear (I_{UO}). An expanded 10-degree of freedom model is then developed. The non-zero natural frequencies (in Hz) for the 3rd gear engaged condition are as follows: 6 (6), 265 (264), (847), 1922 (1930), 2385 (2396), (2646), (5957), 6026 (6053), and (6857); the values in parentheses are from the expanded 10-degree of freedom linear model. Since the maximum deviation of the simplified model is less than 1 % and all torsional mode shapes are well described, it is used for further analyses. The corresponding mode shapes of the 6-degree of freedom model are given in Table 2. All modes have been normalized using the gear ratios that include the following gear radii: headset driver (R_{HI}), headset driven on the counter shaft (R_{HO}), engaged driver (R_{EI}), unloaded driver (R_{UI}), engaged output (R_{EO}), and unloaded output (R_{UO}).

Mode		1	2	3	4	5
Natural Freq. (Hz)		6	265	1922	2385	6026
Flywheel	(θ_F)	-0.0069	0.0000	0.0000	0.0000	0.0000
Clutch hub	(θ_H)	0.9990	1.0000	-0.0104	-0.0014	0.0000
Input shaft	(θ_{IN})	1.0000	-0.8498	1.0000	0.2064	0.0021
Counter shaft	(θ_{CT})	1.0001	-0.9734	-0.1417	-0.1653	0.0231
Engaged	(θ_{EO})	1.0001	-0.9870	-0.5116	1.4583	0.0038
Unloaded	(θ_{UO})	1.0001	-0.9753	-0.1581	-0.1967	1.1242

Table 2: Natural frequency and modes of the 6-degree of freedom model of Figure 1.

Next, various nonlinear elements are defined for the dual-staged clutch (with hysteresis), and all gear pairs (with backlashes at the headset gear pair, engaged gear pair, and unloaded gear pair) within the 6-degree of freedom model. This is designated here as Case A. As shown in Figure 3a, the clutch torque is modeled by two components. The first component defines the dual-staged springs, k_{C1} and k_{C2}, and the second relates torque to the hysteresis of each stage, H_1 and H_2. The gear pair regimes are modeled in terms of mesh force stiffnesses, k_{GH}, k_{GE}, and k_{GU} along the line of action, and gap functions, as depicted in Figures 3b and 3c. All physical discontinuities are conditioned using mathematical smoothing functions [3]. Finally, the governing equations are non-dimensionalized to ensure that the system is not strongly "stiff" [1]. A $4/5^{\text{th}}$ order Runge-Kutta algorithm with a variable time step is used for numerical integration. Typical results yielded by computer simulations are shown in Figures 2 and 3. Single-sided impacts are observed at the unloaded gear pair location (Figure 2). The full contact in the driven side, flat regime around the -0.05 mm line, is relatively short and the unloaded driven gear instantaneously goes back to the floating condition. The unloaded gear starts to affect the driver after 0.58 s, and the impacting period and oscillating displacement then become regular. Gear mesh force plots of figures 3b and 3c show single-sided impacts at both engaged and unloaded pairs. After comparing the relative acceleration levels for the engaged and unloaded gear pairs, the level difference is found to be similar to that seen in vehicle measurements. However, the engaged gear pair does not show any signs of the impact before the rattle from unloaded gear takes place (before 0.58 s). It is observed that relative acceleration at the engaged gear pair starts to show peaks in the regime where unloaded gear rattle is taking place, and minor single-sided impacts at engaged gear are observed in Figure 3b. It is clear that impacts from the unloaded gear pair influence the relative acceleration level of the engaged gear pair, and this explains the acceleration burst of the engaged gear pair at 950 rpm, as measured in the vehicle.

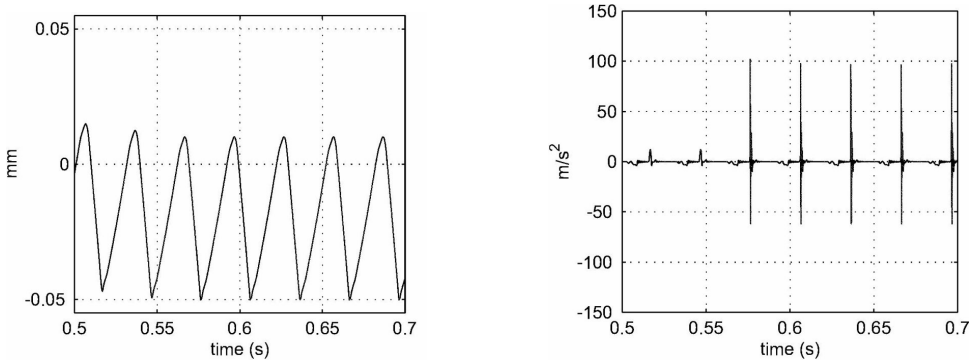

(a): Relative displacement. **(b):** Relative acceleration.

Figure 2: Relative acceleration and displacement of unloaded gear pair (case A).

3 - DESIGN STUDIES

To find possible solutions to the unloaded gear pair rattle, two case studies are carried out. The simulation model of Figure 1 is expanded and simulation results are compared between the baseline and modified cases. First, the application of dual-mass flywheel is considered (designated here as Case B). In the simulation, the flywheel inertia (I_F) is divided into the first and second flywheel masses; values selected are 0.7 I_F and 0.3 I_F. The main design parameters are the first stage stiffness (k_{C1}) and interfacial friction (H_1) as shown in Figure 4a. The stiffness of the dual-mass flywheel is usually lower than k_{C1}. For the sake of this study, the flywheel stiffness is assumed equal to k_{C1} of the single-mass flywheel model.

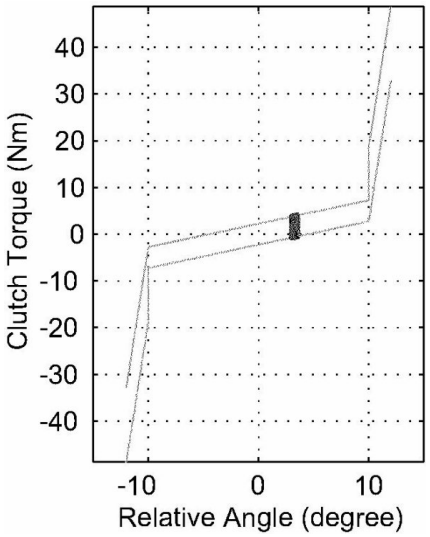

(a): Dual-stage clutch torque.

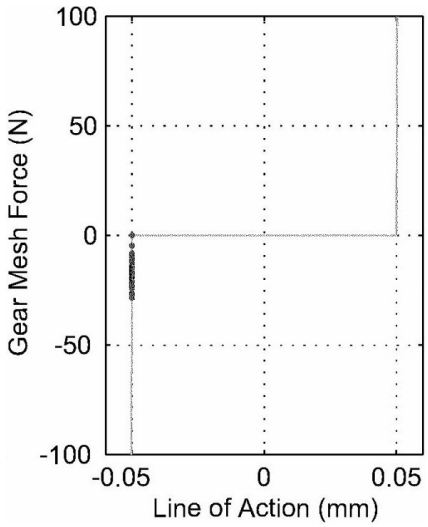

(b): Engaged gear mesh force.

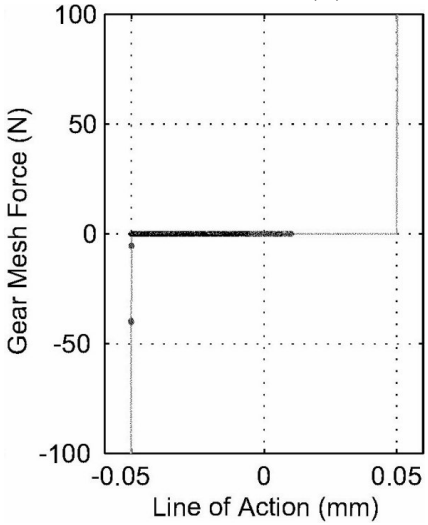

(c): Unloaded gear mesh force.

Figure 3: Clutch torque and gear mesh forces (case A).

Then, the new k'_{C1} is increased to $6k_{C1}$. The associated hysteresis is often nonlinear and its sign is related to the direction of relative velocity between the first and second flywheel masses. Previously seen single-sided impacts are not observed anymore; instead, low frequency vibrations due to the compliant spring of dual-mass flywheel take place as shown in Figure 4b. This demonstrates that the dual-mass flywheel isolates torsional excitations as seen in Figure 4a.

Next, the effect of drag torque (T_D) is analyzed (designated here as Case C). The direction of drag torque between the unloaded driven gear and the output shaft T_{D4}, as shown in Figure 1, can be defined by three conditions. First, the main shaft rotates faster than the unloaded gear. In this case, the drag actually pulls the unloaded gear along and makes it more likely to lose contact with the driving gear. Second, the converse occurs when the main shaft runs slower than the unloaded gear. Third, the main shaft and the unloaded gear rotate at the same speed. There would be no drag torque effects for this rare case. In practical transmissions, the drag between the main shaft and unloaded gear may be minimized so as to increase the energy efficiency. However, low drag can initiate impact favorable conditions when the unloaded gear is about to lose contact. Comparison of the relative acceleration levels between low and high T_{D4} is shown in Figure 5 and some reduction in single-sided impacts for the higher drag torque case is witnessed in Figure 5b. The time taken to reach steady state or to lose contact is governed by T_{D4}. If the drag is small, the unloaded driven gear goes into the steady state condition immediately after the contact (around 0.58 s in Figure 5a). Conversely, if the drag is high, the floating action can be suppressed by the drag and the transition time gets longer (from 0.58 to 0.66 s in Figure 5b).

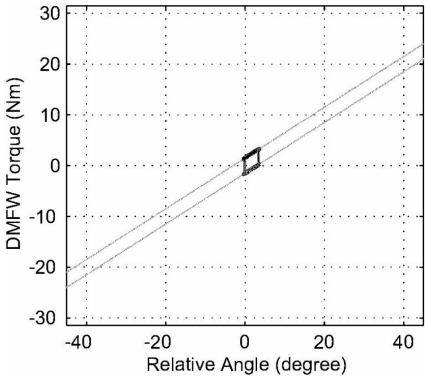

(a): Dual-mass flywheel torque.

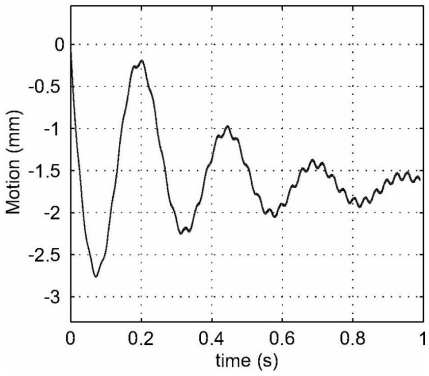

(b): Low frequency component.

Figure 4: Effect of dual-mass flywheel on results (case B).

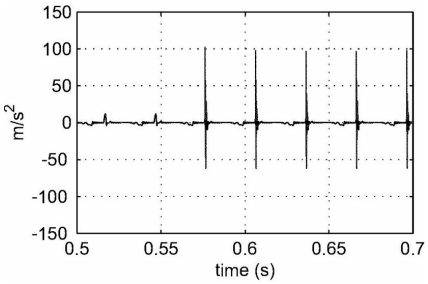

(a): With low drag torque.

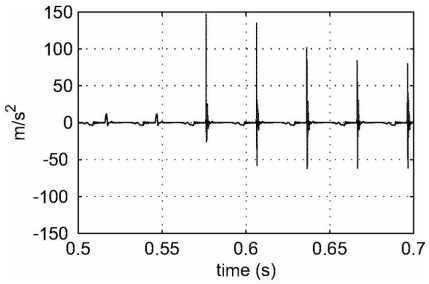

(b): With high drag torque.

Figure 5: Effect of drag torque on the motion of unloaded gear pair (case C).

4 - CONCLUSION

From the linear analysis, it is clear that the reduced 6-degree of freedom model can effectively represent the manual transmission since natural modes show excellent agreement with expanded models. Furthermore, mode maps based on the equivalent stiffness concept [2] show similar curves. Therefore, the model of Figure 1 can be used for nonlinear analyses. Dynamic interactions between unloaded gear rattle and engaged gear acceleration seem to depend upon the drag torque (T_{D3}), counter shaft and driver gear inertia (I_{CT}), and engaged gear inertia (I_{EO}), according to computer simulation studies.

From the linear analysis, it is clear that the reduced 6-degree of freedom model can effectively represent the manual transmission since natural modes show excellent agreement with expanded models. Furthermore, mode maps based on the equivalent stiffness concept [2] show similar curves. Therefore, the model of Figure 1 can be used for nonlinear analyses. Dynamic interactions between unloaded gear rattle and engaged gear acceleration seem to depend upon the drag torque (T_{D3}), counter shaft and driver gear inertia (I_{CT}), and engaged gear inertia (I_{EO}), according to computer simulation studies.

Application of a dual-mass flywheel eliminates the impacts in the unloaded gear pair. Therefore, the impacts in the engaged gear pair are also eliminated. This has been previously seen for the engaged gear rattle problems, but the dual-mass flywheel also seems to work in controlling the unloaded gear pair rattle case. Nonetheless, a possible drawback is observed since it introduces low frequency oscillations in Figure 4b. This component comes from the compliant spring of the dual-mass flywheel (Figure 4a). When the drag torque is very high, the relative acceleration levels decrease but the rattle-like condition still persists. Therefore, an oil-sealed bearing could be introduced to control only for light unloaded gear rattle problems; however, it may not be a fundamental solution to many rattle problems. Qualitative comparisons between experimental measurements and simulation predictions are valid, but more quantitative studies need to be performed. Work in progress will carefully examine relationships between controlling parameters and dynamic interactions between sub-systems.

ACKNOWLEDGEMENTS

We wish to acknowledge the "gear rattle" consortium members, Eaton R & D, Eaton Clutch, Fiat CRF, LuK, Saab, and Volvo Trucks for supporting this research.

REFERENCES

1. **R. Singh, H. Xie, and R. J. Comparin**, Analysis of Automotive Neutral Gear Rattle, *Journal of Sound and Vibration*, Vol. 131, pp. 177-196, 1989

2. **C. Padmanabhan, R. C. Barlow, T. E. Rook, and R. Singh**, Computational Issues Associated with Gear Rattle Analysis, *Journal of Mechanical Design*, Vol. 117, pp. 185-192, 1995

3. **E. P. Trochon**, *Analytical Formulation of Automotive Drivetrain Rattle Problems*, M.S. Thesis, The Ohio State University, 1997